ACS APPLIED MATERIALS & INTERFACES

www.acsami.org

Research Article

Self-Assembled Mechanochromic Shape Memory Photonic Crystals by Doctor Blade Coating

Chia-Hua Hsieh, Yi-Cheng Lu, and Hongta Yang*

Cite This: *ACS Appl. Mater. Interfaces* 2020, 12, 36478–36484

Read Online

ACCESS | Metrics & More | Article Recommendations | Supporting Information

ABSTRACT: Mechanochromic shape memory photonic crystals can memorize their original structures and recover the inherent structural colors in response to external stimuli; thereby they have rendered various important optical applications. Unfortunately, most existing shape memory polymers are thermoresponsive, and the corresponding mechanochromic characteristics are limited by the heat-demanding programming process. Besides that, a great majority of current fabrication methodologies suffer from low throughput, hindering the practical applications. Herein, a scalable technology is developed to engineer macroporous shape memory photonic crystals by self-assembling silica colloidal crystals in a polyurethane acrylate/polyethoxylated trimethylolpropane triacrylate/poly(ethylene glycol) diacrylate matrix, followed by a wet etching treatment to selectively remove silica colloids. The as-created photonic crystals display a brilliant structural color, which is reversibly tunable with mechanical deformation at ambient conditions. Upon stretching, the reduced interlayer lattice spacing of the photonic crystals leads to a blueshift of the reflection peak position and a significant color change. Importantly, the stretched macroporous film can fix its temporary structures without applying any contact force and simultaneously recover its original configuration and appearance by applying ethanol evaporation-induced capillary pressures. The reversibility and the dependence of templated silica colloid size on mechanochromic characteristics have also been investigated in the research.

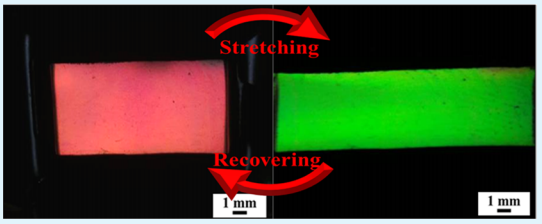

KEYWORDS: *mechanochromic, shape memory, photonic crystals, self-assembly, reversibility*

INTRODUCTION

Photonic crystals are periodically arranged structures possessing a photonic band gap, which forbids certain wavelength ranges of electromagnetic waves from propagating through.[1] The photonic stop band, generally determined by the refractive index and interlayer lattice spacing of photonic crystals, induces the formation of structural colors and provides tremendous opportunities in manipulating light flow. The tunable optical properties and flamboyant visual effects therefore can be controlled by structure deformation. Take one preeminent example: mechanochromic photonic crystals are capable of changing their intrinsic optical properties in response to external mechanical stimuli either permanently or reversibly.[2] Owning to the strain-induced color change characteristic, the mechanochromic materials reliably display visual signals of mechanical pressures and strains, leading to increasing interests for a large variety of applications in mechanical sensing, response optical devices, biometric materials, security device, and anticounterfeiting field.[3−7]

Taking advantage of fast mechanochromic response, photonic gels have already been well explored in the past decade.[8−11] Charged colloids can be spontaneously assembled in a liquid medium, caused by electrostatic repulsion between colloids, and then embedded in a solvent-swollen gel. Even though the elastic matrix is highly stretchable, the photonic gel suffers from low optical saturation performance and poor mechanical stability against stretching. It shall be noted that the flexibility of the photonic gel can be improved by introducing porous structures.[12,13] Nevertheless, almost all the reported inverse opal gels are limited by time-consuming procedures of fabrication and poor durability in repeated usage. Moreover, solvent vaporization during stretching makes gels only suitable for short-term use in restricted environments. Thus, liquid-free elastic photonic crystals with fast, durable, and reversible mechanochromic response remain an urgent yet unmet demand.

To tackle the challenge, spontaneously crystallized colloidal crystals have been extensively utilized as templates for developing polymer-based photonic crystals.[14−16] Although the polymeric composites perform durable and reversible color changes in response to external mechanical forces, the color transform range is restricted, and hysteresis is inevitable because the extension entails considerable rearrangement of

Received: April 22, 2020
Accepted: July 16, 2020
Published: July 16, 2020

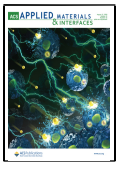

https://dx.doi.org/10.1021/acsami.0c07410
ACS Appl. Mater. Interfaces 2020, 12, 36478–36484

colloids. In addition, limited by low refractive index contrast between inelastic colloids and elastic polymeric matrix, most of the reported composites are translucent and only allow low color saturation. By contrast, macroporous photonic crystals show much less resistance against mechanical deformation and thus deliver a larger color transform range.[17,18] In spite of this, the low mechanical stability of macroporous structures renders milky color during deformation, reducing color saturation and greatly restricting practical applications.[19] Alternatively, shape memory polymers are synthesized and proposed to improve the mechanical stability.[20−22] Macroporous shape memory photonic crystals can be facilely deformed above the glass transition temperature and cooled below the temperature to memorize the temporary structures. Shape recovery occurs once the materials are reheated, whereas polymer chain mobility increases and allows the materials to recover their original configurations and appearances.[23] Unfortunately, the mechanochromic characteristics of the thermoresponsive shape memory polymers are limited by the heat-demanding programming process.

Apart from that, high-throughput fabrication of photonic crystals is another challenge that needs to be addressed. In recent decades, a number of top-down lithography-based technologies and bottom-up self-assembly approaches have been developed to fabricate photonic crystals.[24−27] Compared to complex lithographic technologies, which involve exorbitant and sophisticated equipment, colloidal self-assembly approaches utilize self-assembled colloidal crystal-based structural templates for creating photonic crystals. Even though the template-based methodologies are relatively simple and inexpensive, most of the current self-assembled photonic crystals suffer from low throughput and can only be elaborately fabricated.[28] The drawbacks greatly impede their applications.

To address these issues, this research exploits a roll-to-roll compatible doctor blade coating technique to self-assemble macroporous shape memory photonic crystals. The coating technique is widely used in fabricating thin films over large areas.[29,30] Owing to a wide range of coating solutions, low solution wastage, and high-throughput coating speed, the technique can easily be scaled up from development to manufacture. Importantly, the as-designed shape memory polymer enables mechanical deformation and shape recovery at room temperature. Instead of heat, shape memory programming is induced by applying external mechanical stimuli, while the shape memory recovery can be achieved by introducing ethanol evaporation-induced capillary pressure. The novel mechanochromic shape memory photonic crystals are mechanically robust, highly reversible, and easily scalable, leading to perceivable monitoring by readable optical signals.

EXPERIMENTAL SECTION

Materials. The reagents employed to synthesize silica particles, including tetraethyl orthosilicate (TEOS, 98%), absolute ethanol (99%), and ammonium hydroxide (28%), were acquired from Sigma-Aldrich Co. Commercial UV-curable urethane acrylate (UA, ETERANE 8928) oligomers, UV-curable ethoxylated trimethylolpropane triacrylate (ETPTA, SR 415) oligomers, and UV-curable ethylene glycol diacrylate (EGDA, SR 610) oligomers were provided by Eternal Materials Co. Ltd., Taiwan and Sartomer Co., respectively. 2-Hydroxy-2-methyl-1-phenyl-1-propanone (HMPP, Darocur 1173), which served as a photoinitiator, was obtained from BASF Co., Germany. Hydrofluoric acid (HF, 48%) was purchased from Merck KGaA Co., Germany. All the chemicals were of reagent quality and used directly as received. Deionized water (17.8 MΩ cm) was purified in a Millipore A-10 water purification system.

Preparation of UV-Curable Silica Particle Dispersions. Monodispersed spherical silica particles with diameters of 250, 330, and 370 nm were synthesized in a sol−gel process developed by Werber Stöber.[31] The Stöber silica particles were washed with absolute ethanol by five centrifugation (7000 rpm for 15 min) and redispersion (5 min probe ultrasonication) cycles to completely eliminate unreacted chemicals and any other byproducts, followed by dispersing in a viscous oligomer mixture containing UV-curable UA oligomers, UV-curable EGDA oligomers, UV-curable ETPTA oligomers, and 1 vol % photoinitiator using a 700 watt probe ultrasonicator for 10 min. The silica particle volume fraction was 74 vol % in the dispersion, in which the volume ratio of UA oligomers, EGDA oligomers, and ETPTA oligomers was controlled to be 7:2:1. Benefiting from the previous work, the volume ratio of EGDA oligomers and ETPTA oligomers was adjusted to be 2:1 in this research.[22,23] To improve the elasticity and mechanical stability of the materials, UA oligomers were introduced, in which the volume fraction of UA oligomers was 70%. For lower volume fraction of UA oligomers, the as-prepared materials possessed a high stiffness and greatly restricted the mechanochromic characteristics. On the contrary, for higher volume fraction of UA oligomers, the materials were not able to memorize the temporary structures.

Self-Assembled Macroporous Photonic Crystals by Doctor Blade Coating. In the self-assembling process, a double-edged razor blade (Fisher Scientific Inc.) was vertically positioned across a 1 × 3 in.^{2} plain glass microscope slide (Corning Inc.), which had been coated with a PUA/PEGDA/PETPTA wetting layer. For the wetting layer, the volume ratio of PUA, PEGDA, and PETPTA was 7:2:1. After dispensing the as-prepared silica particle dispersion onto the glass substrate, the substrate was dragged underneath the blade at a constant speed of 5 mm/min using a KD Scientific syringe pump. The coating speed ranging from 1 to 20 mm/min can be controlled by regulating the motor speed of the syringe pump. In the coating process, the immobilized blade can spread the dispersion onto the substrate uniformly and render a unidirectional shear force to assemble the silica particles in the dispersion. The oligomer mixture was then photopolymerized under UV radiation in a UV curing chamber (X Lite 500, OPAS) to produce a silica colloidal crystal/shape memory polymer composite. In general, higher coating speed results in a thicker coated polymer composite. In addition, the composite thickness also depends on the gap size, wetting behavior, and rheological properties of the dispersion.[32] The embedded silica particles were finally wet-etched in a 2 vol % HF ethanol-based solution to create macroporous shape memory photonic crystals.

Characterization. The photographic images of the macroporous shape memory photonic crystals were taken using a digital camera (Canon SX720). The surface morphologies of the specimens were performed by a scanning electron microscope (JEOL 6335F). Platinum layers were sputter-deposited onto the specimens prior to imaging. Optical reflection spectra were carried out using a high-resolution fiber-optic UV−visible−near-IR spectrometer (Ocean Optics HR4000) with a deuterium tungsten halogen light source (Ocean Optics DT-MINI-2). Ocean Optics Spectroscopy software was employed to record the spectra in the wavelength range from 400 to 800 nm. The tensile stress−elongation relations of the specimens were examined by an electromechanical tensile strength testing machine (GOTECH Al-3000).

RESULTS AND DISCUSSION

A simplified doctor blade coating process for self-assembling macroporous shape memory photonic crystals is schematically illustrated in Figure 1. Monodispersed Stöber silica particles are dispersed in an oligomer mixture, containing UA oligomers, EGDA oligomers, and ETPTA oligomers, with HMPP as a photoinitiator. The as-prepared silica particle dispersion is dispensed on a PUA/PEGDA/PETPTA-coated glass substrate, while an immobilized razor blade is introduced

https://dx.doi.org/10.1021/acsami.0c07410
ACS Appl. Mater. Interfaces 2020, 12, 36478−36484

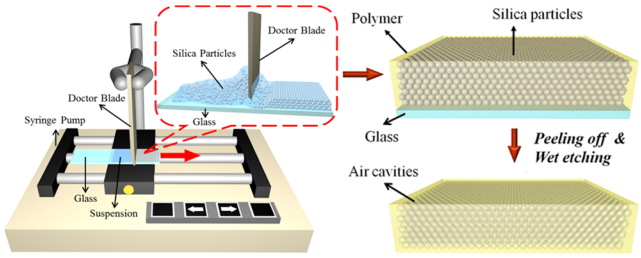

Figure 1. Schematic illustration of the experimental procedures for self-assembling mechanochromic photonic crystals using a scalable doctor blade coating technology.

to align silica particles as the glass substrate is dragged using a syringe pump. As reported in our previous work, the colloidal crystallization in the coating process is attributed to shear-induced ordering.[32,33] The shear-thinning behavior of the silica particle dispersion is caused by the reduced resistance as ordered silica particle layers glide over each other. Importantly, the shear rate resulted from the dragged substrate is less than the critical shear rate demanded to attain the relative viscosity plateau, indicating that the shear-induced crystallization of silica particles is also determined by the pressure-driven flow. The oligomers are then photopolymerized to develop a silica colloidal crystal/shape memory polymer composite film. Even though a few defects can be found, most of the shear-aligned silica particles are three-dimensionally close-packed (Figure 2).

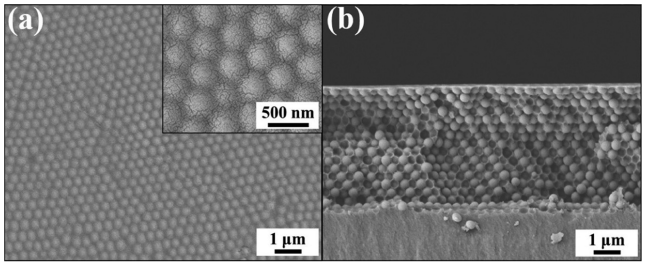

Figure 2. Colloidal crystal/shape memory polymer composites fabricated by the doctor blade coating technology. (a) Top-view scanning electron microscopy (SEM) image of a composite consisting of 370 nm silica colloid crystals coated on a glass substrate. The inset shows a magnified SEM image. (b) Cross-sectional SEM image of the sample in (a).

After peeling off the composite film, the silica particles embedded in the polymeric matrix are completely removed using an HF ethanol-based solution to engineer free-standing macroporous shape memory photonic crystals. As revealed in Figure 3a, the macroporous film templated from 370 nm silica colloidal crystals displays a sticking red color. The uniform color is attributed to Bragg diffraction from long-range highly ordered air cavities in the polymeric matrix, as disclosed in Figure 3b–d. Importantly, the three-dimensional hexagonal close-packed lattice can be well reserved during the wet etching treatment.

To characterize the mechanochromic properties of the as-fabricated macroporous shape memory photonic crystals, a fiber-optic spectrometer is employed to evaluate the normal incidence optical reflection spectra of the macroporous film under various uniaxial elongation ratios. As revealed in Figure 4a, the reflection peak position of the unstretched macroporous film templated from 370 nm silica colloidal crystals locates at 654 nm (black curve), agreeing well with the

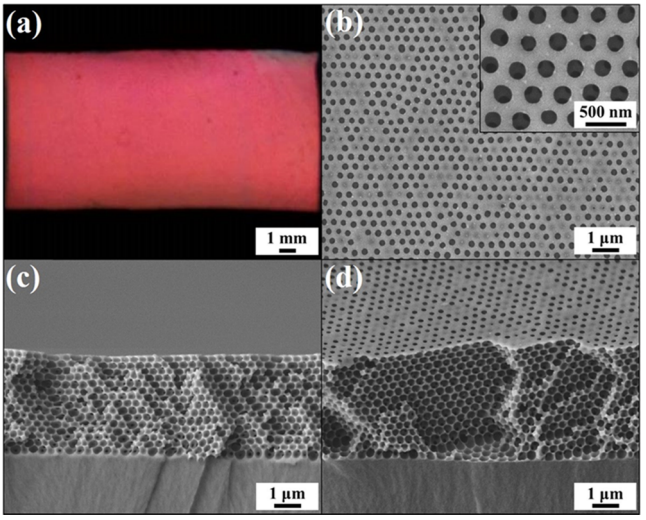

Figure 3. Macroporous shape memory polymer films after the selective removal of silica particles. (a) Photographic image of a free-standing macroporous film templated from 370 nm silica colloidal crystals. (b) Top-view SEM image of the sample in (a). The inset shows a magnified SEM image. (c) Cross-sectional SEM image of the sample in (a). (d) Tilted-view SEM image of the sample in (a).

theoretical peak position (657 nm) estimated according to Bragg's equation

$$\lambda_{peak} = 2n_{eff}\, d \sin\theta$$

where n_{eff}, d, and θ represent the effective refractive index of the medium, the interlayer lattice spacing, and the incidence angle, respectively.[34] The result discloses the highly crystalline quality of the three-dimensional hexagonal close-packed macroporous photonic crystals. In addition, the large refractive index difference between the polymer and air leads to a high reflection amplitude (92%). Interestingly, the reflection peak position can be gradually changed, while the macroporous film is stretched uniaxially. As illustrated in Figure S1, the stretching reduces the thickness and the interlayer lattice spacing (d) of the film, thereby causing the peak position continuously shift from 654 to 546 nm as the elongation rate of film increases to 50%. It is worth mentioning that the peak position is in a linear relationship with the elongation rate (Figure 4b). The structural change and the corresponding blueshift of the macroporous photonic crystals can further be interpreted by a combination of Bragg's equation and Poisson's effect

$$\lambda_{peak} = 2n_{eff}\, d(1 - \nu\varepsilon) \sin\theta$$

where d indicates the interlayer lattice spacing of the unstretched film, ν denotes Poisson's ratio, and ε represents the elongation ratio of the film along the lateral direction.[35] Assuming that the effective refractive index of the film (n_{eff}) remains the same in the whole stretching process, the peak position (λ_{peak}) shift after stretching is therefore proportional to the elongation ratio. In comparison with swollen opals, organic gels, or hydrogels, the self-assembled macroporous film significantly allows high extensionality (70%), as disclosed in Figure S2.[36−38] It is also worth noting that the strength of the reflection only slightly reduces during the stretching.

As displayed in Figure 5a, the macroporous shape memory film exhibits a uniform red color with high color saturation. Upon stretching, the color obviously changes with the elongation ratio and turns into green color as the elongation

https://dx.doi.org/10.1021/acsami.0c07410
ACS Appl. Mater. Interfaces 2020, 12, 36478−36484

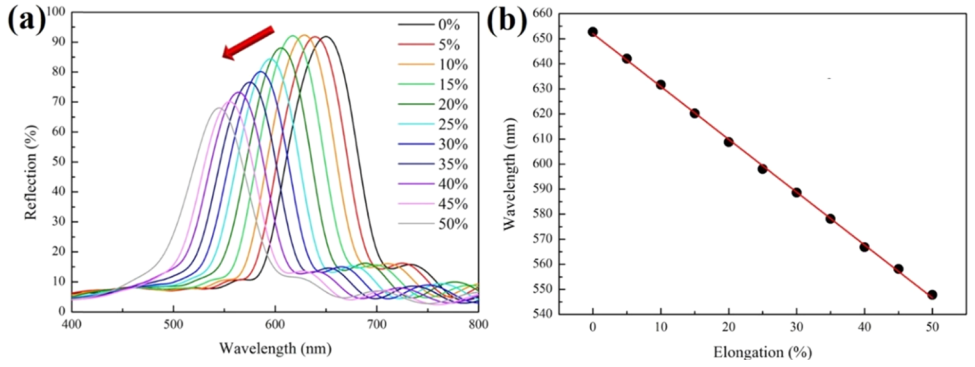

Figure 4. (a) Normal incidence optical reflection spectra of the macroporous shape memory polymer film templated from 370 nm silica colloidal crystals under various elongation ratios from 0% (black) to 50% (gray). (b) Dependence of the optical reflection peak position on the elongation ratio.

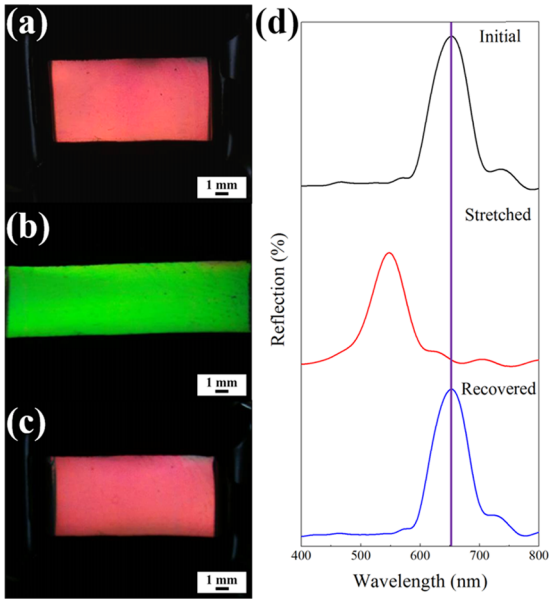

Figure 5. Photographic images of (a) the unstretched macroporous shape memory polymer film templated from 370 nm silica colloidal crystals, (b) the macroporous film in a stretched state (elongation ratio = 50%), and (c) the macroporous film in a recovered state. (d) Normal incidence optical reflection spectra of the macroporous film in an unstretched state (black curve), a stretched state (red curve), and a recovered state (blue curve).

ratio reaches 50% (Figures S3 and 5b). Although a few discolorations near the edges of the film are found due to defects caused by handling during the stretching, the color and the color saturation remain consistent. Interestingly, the macroporous film can permanently maintain the temporary stretched structures and perform a brilliant color without applying any contact force at 25 °C and a relative humidity of 30%. The shape memory characteristics result from the energy transformation between the external energy and the internal energy change of the shape memory polymer, which behaves like an elastic material at room temperature.[39] The applied tensile stress therefore overcomes the shape memory activation barrier and deforms the original crystalline lattice of the macroporous photonic crystals during the stretching process. To activate the outstretched polymer chain mobility and trigger the temporary crystalline lattice recovery, external energy is evidently required. More interestingly, the film recovers its original length and red color once again as the film is immersed in absolute ethanol, followed by drying out of ethanol at 25 °C (Figures S3 and 5c). The ethanol evaporation-induced capillary pressure squeezes the outstretched polymer chains and recovers the elastic polymeric matrix into its original configuration. Besides ethanol, a diverse range of low surface tension solvents, such as toluene and acetone, can be applied for the structure recovery and the corresponding color change. The SEM images in Figure S4 verify the conjecture, as the three-dimensional hexagonal close-packed crystalline lattice is displayed.

To further confirm the mechanochromic shape memory properties, the optical reflection spectra of the macroporous film in an unstretched state, a stretched state, and a recovered state are estimated (Figure 5d). Clearly, the reflection peak position and the peak intensity of the recovered film agree well with those of the unstretched film, revealing that the temporarily deformed crystalline lattice can be fully recovered. Importantly, the shape memory deformation and recovery processes are completely reversible. At room temperature, the macroporous shape memory film can be deformed and recovered at least for 25 cycles without any failure and noticeable change in reflection peak position (Figure 6). The corresponding peak position is shifted between 654 and 546 nm reversibly in the absence of a hysteresis. The highly elastic

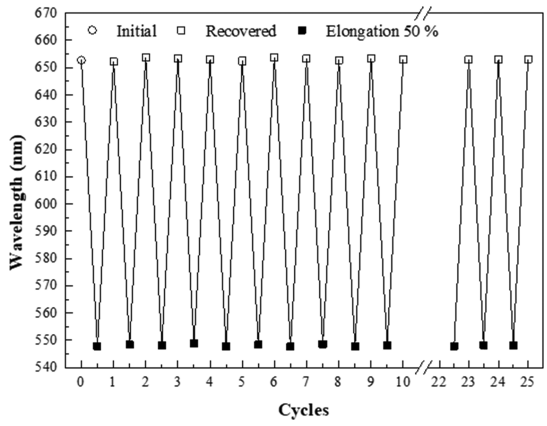

Figure 6. Reversible optical reflection peak position shift of the macroporous shape memory polymer film templated from 370 nm silica colloidal crystals between the stretched state with elongation ratio = 50% (white squares) and the recovered state (black squares) for 25 cycles.

https://dx.doi.org/10.1021/acsami.0c07410
ACS Appl. Mater. Interfaces 2020, 12, 36478−36484

shape memory macroporous photonic crystals feature a great reusability and stable mechanochromic properties, which are comparable with mechanochromic materials previously reported.[40,41]

The interlayer lattice spacing effect on the mechanochromic characteristics of the macroporous photonic crystals is also investigated in this research. Macroporous shape memory photonic crystals templated from 330 nm silica colloidal crystals and 250 nm silica colloidal crystals are fabricated by the doctor blade coating technology. As demonstrated previously, a homogeneous yellow macroporous film is derived from Bragg's diffraction of the three-dimensional hexagonal close-packed 330 nm air cavities in the polymeric matrix (Figure S5). Upon stretching uniaxially, the reflection peak position is gradually shifted from 582 to 487 nm as the elongation rate of film reaches 50%, whereas a wavelength shift of 95 nm is achieved. It is worth pointing out that the reflection peak position blueshifts linearly with the increase of the elongation rate. The corresponding structural color therefore turns into greenish-blue (Figure 7). Ethanol

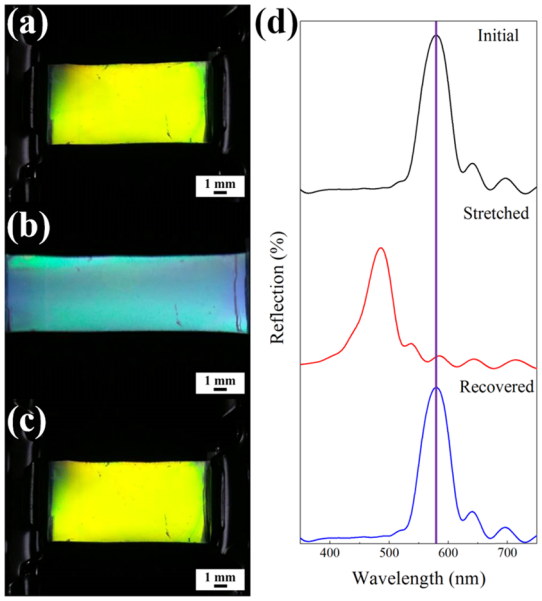

Figure 7. Photographic images of (a) the unstretched macroporous shape memory polymer film templated from 330 nm silica colloidal crystals, (b) the macroporous film in a stretched state (elongation ratio = 50%), and (c) the macroporous film in a recovered state. (d) Normal incidence optical reflection spectra of the macroporous film in an unstretched state (black curve), a stretched state (red curve), and a recovered state (blue curve).

evaporation-induced capillary pressures can then be introduced to recover the original configuration and to change the color. Apparently, the recovered peak position matches well with the initial one, indicating the shape memory characteristics. In addition, the color change is reversible for at least 25 cycles without any nonfulfillment (Figure S6). Importantly, the structural color changes under compression and turns into carol red as the compressive strain reaches −50%, while the original color can be recovered after applying ethanol evaporation-induced capillary pressures (Figure S7).

Similarly, hexagonal close-packed 250 nm air cavities in the macroporous photonic crystals are capable of reflecting violet light (Figure S8). Interestingly, as the macroporous film is uniaxially stretched until the elongation ratio reaches 50%, the color dramatically changes from violet to transparent (Figure 8a,b), while the corresponding reflection peak position linearly

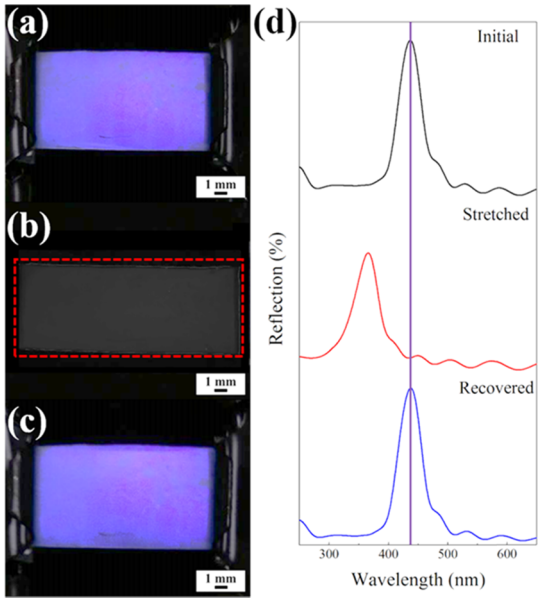

Figure 8. Photographic images of (a) the unstretched macroporous shape memory polymer film templated from 250 nm silica colloidal crystals, (b) the macroporous film in a stretched state (elongation ratio = 50%), and (c) the macroporous film in a recovered state. (d) Normal incidence optical reflection spectra of the macroporous film in an unstretched state (black curve), a stretched state (red curve), and a recovered state (blue curve).

shifts from 439 to 368 nm under the increasing elongation ratio (Figure S6e,f). The stretched macroporous film (elongation ratio = 50%) can reflect ca. 66% incident ultraviolet radiation and less than 3% incident visible light; thereby the stretched film features high transparency. The results suggest that it is valid to engineer a naked-eye detector for mechanical forces by controlling the interlayer lattice spacing of the macroporous photonic crystals. In addition, the color can be reversibly changed for 25 cycles by applying ethanol evaporation-induced capillary pressures (Figure S9). Importantly, the reflection peak position shift range of the as-fabricated macroporous photonic crystals is proportional to the interlayer lattice spacing, whereas the wavelength shifts between the unstretched state and stretched state (elongation ratio = 50%) of the macroporous films templated from 370, 330, and 250 nm silica colloidal crystals are 108, 95, and 71 nm, respectively. With a consistent Poisson's ratio (ν), a larger interlayer lattice spacing results in a larger blueshift while the macroporous shape memory film is stretched, leading to a noticeable color change.

CONCLUSIONS

In summary, a scalable doctor blade coating technology is developed to engineer free-standing and flexible macroporous shape memory photonic crystals, which allows a high extensionality of up to 70%. Upon stretching uniaxially, the reduced interlayer lattice spacing of the macroporous photonic crystals leads to a noticeable blueshift of the reflection peak position and an obvious color change with high color saturation. It is worth mentioning that the macroporous film

https://dx.doi.org/10.1021/acsami.0c07410
ACS Appl. Mater. Interfaces 2020, 12, 36478−36484

templated from larger silica colloids causes a larger blueshift, resulting in a noticeable color change. Interestingly, the stretched macroporous film can memorize its temporary structure without applying any contact force and instantaneously recovers its original configuration and appearance under ambient conditions by introducing ethanol evaporation-induced capillary pressures. The shape deformation and recovery cycles exhibit reversible responses and can be repeated for at least 25 cycles. The robust and durable macroporous film features high-quality mechanochromic behaviors and shape memory characteristics, which promote a great potential for practical applications in optical sensor materials, smart optical display units, novel biometric materials, and anticounterfeiting fields.

■ ASSOCIATED CONTENT

Supporting Information

The Supporting Information is available free of charge at https://pubs.acs.org/doi/10.1021/acsami.0c07410.

Schematic illustration of the stretching process, relationship of tensile stress and elongation ratio, photos, SEM images, normal incidence optical reflection spectra, dependence of optical reflection peak position on elongation ratio, and reversible optical reflection peak position shifts of macroporous shape memory polymer films (PDF)

■ AUTHOR INFORMATION

Corresponding Author

Hongta Yang − *Department of Chemical Engineering, National Chung Hsing University, Taichung City 40227, Taiwan;* orcid.org/0000-0002-5822-1469; Email: hyang@dragon.nchu.edu.tw

Authors

Chia-Hua Hsieh − *Department of Chemical Engineering, National Chung Hsing University, Taichung City 40227, Taiwan*

Yi-Cheng Lu − *Department of Chemical Engineering, National Chung Hsing University, Taichung City 40227, Taiwan*

Complete contact information is available at: https://pubs.acs.org/10.1021/acsami.0c07410

Notes

The authors declare no competing financial interest.

■ ACKNOWLEDGMENTS

Acknowledgment is made to the National Science Council under MOST 108-2221-E-005-038-MY2 and MOST 108-2221-E-005-040 for financial support.

■ REFERENCES

(1) Teyssier, J.; Saenko, S. V.; Van Der Marel, D.; Milinkovitch, M. C. Photonic Crystals Cause Active Colour Change in Chameleons. *Nat. Commun.* **2015**, *6*, No. 6368.

(2) Sun, X.; Zhang, J.; Lu, X.; Fang, X.; Peng, H. Mechanochromic Photonic-Crystal Fibers Based on Continuous Sheets of Aligned Carbon Nanotubes. *Angew. Chem., Int. Ed.* **2015**, *54*, 3630−3634.

(3) Zhang, R.; Wang, Q.; Zheng, X. Flexible Mechanochromic Photonic Crystals: Routes to Visual Sensors and Their Mechanical Properties. *J. Mater. Chem. C* **2018**, *6*, 3182−3199.

(4) Lee, G. H.; Choi, T. M.; Kim, B.; Han, S. H.; Lee, J. M.; Kim, S.-H. Chameleon-Inspired Mechanochromic Photonic Films Composed of Non-Close-Packed Colloidal Arrays. *ACS Nano* **2017**, *11*, 11350−11357.

(5) Jia, X.; Wang, J.; Wang, K.; Zhu, J. Highly Sensitive Mechanochromic Photonic Hydrogels with Fast Reversibility and Mechanical Stability. *Langmuir* **2015**, *31*, 8732−8737.

(6) Li, H.; Sun, X.; Peng, H. Mechanochromic Fibers with Structural Color. *ChemPhysChem* **2015**, *16*, 3761−3768.

(7) Howell, I. R.; Li, C.; Colella, N. S.; Ito, K.; Watkins, J. J. Strain-Tunable One Dimensional Photonic Crystals Based on Zirconium Dioxide/Slide-Ring Elastomer Nanocomposites for Mechanochromic Sensing. *ACS Appl. Mater. Interfaces* **2015**, *7*, 3641−3646.

(8) Zhao, P.; Li, B.; Tang, Z.; Gao, Y.; Tian, H.; Chen, H. J. S. M. Structures, Stretchable Photonic Crystals with Periodic Cylinder Shaped Air Holes For Improving Mechanochromic Performance. *Smart Mater. Struct.* **2019**, *28*, No. 075037.

(9) Cho, Y.; Lee, S. Y.; Ellerthorpe, L.; Feng, G.; Lin, G.; Wu, G.; Yin, J.; Yang, S. Elastoplastic Inverse Opals as Power-Free Mechanochromic Sensors for Force Recording. *Adv. Funct. Mater.* **2015**, *25*, 6041−6049.

(10) Lee, G. H.; Han, S. H.; Kim, J. B.; Kim, J. H.; Lee, J. M.; Kim, S.-H. Colloidal Photonic Inks for Mechanochromic Films and Patterns with Structural Colors of High Saturation. *Chem. Mater.* **2019**, *31*, 8154−8162.

(11) Zhang, P.; Shi, X. Y.; Schenning, A.; Zhou, G. F.; de Haan, L. T. A Patterned Mechanochromic Photonic Polymer for Reversible Image Reveal. *Adv. Mater. Interfaces* **2020**, *7*, No. 1901878.

(12) Wen, T.; Zhou, X. P.; Zhang, D. X.; Li, D. Luminescent Mechanochromic Porous Coordination Polymers. *Chem. - Eur. J.* **2014**, *20*, 644−648.

(13) Park, J.; Lee, Y.; Barbee, M. H.; Cho, S.; Cho, S.; Shanker, R.; Kim, J.; Myoung, J.; Kim, M. P.; Baig, C.; Craig, S. L.; Ko, H. A Hierarchical Nanoparticle-in-Micropore Architecture for Enhanced Mechanosensitivity and Stretchability in Mechanochromic Electronic Skins. *Adv. Mater.* **2019**, *31*, No. 1808148.

(14) Lin, Z. Z.; Li, L.; Fu, G. Y.; Lai, Z. Z.; Peng, A. H.; Huang, Z. Y. Molecularly Imprinted Polymer-Based Photonic Crystal Sensor Array for The Discrimination of Sulfonamides. *Anal. Chim. Acta* **2020**, *1101*, 32−40.

(15) Chen, D.; Yao, Y.; Wang, Y. M.; Fu, Y.; Zheng, J. Q.; Zhou, H. M. Integrated Outstanding Precision and Mechanical Performance of Transparent 3D Photonic Crystal Devices Employing Cross-Linked Nanospheres via Thermoforming in a Rubbery state. *J. Mater. Chem. C* **2020**, *8*, 2993−2999.

(16) Lin, J. D.; Zhang, Y. S.; Lee, J. Y.; Mo, T. S.; Yeh, H. C.; Lee, C. R. Electrically Tunable Liquid-Crystal-Polymer Composite Laser with Symmetric Sandwich Structure. *Macromolecules* **2020**, *53*, 913−921.

(17) Chen, K.; Zhang, Y. X.; Ge, J. P. Highly Invisible Photonic Crystal Patterns Encrypted in an Inverse Opaline Macroporous Polyurethane Film for Anti-Counterfeiting Applications. *ACS Appl. Mater. Interfaces* **2019**, *11*, 45256−45264.

(18) Liu, Y.; Li, W.; Ding, Z.; Li, Q. J.; Wang, X.; Liu, J.; Zhuo, S. Q.; Shao, R.; Ling, Q. Q.; Zheng, T. S.; Li, J. L. Three-Dimensional Ordered Macroporous Magnetic Photonic Crystal Microspheres for Enrichment and Detection of Mycotoxins (II): The Application in Liquid Chromatography with Fluorescence Detector for Mycotoxins. *J. Chromatogr. A* **2019**, *1604*, No. 460475.

(19) Cardador, M. D.; Garcia, D. S.; Deriziotis, I.; Garin, M.; Llorca, J.; Rodriguez, A. Empirical Demonstration of CO_2 Detection Using Macroporous Silicon Photonic Crystals as Selective Thermal Emitters. *Opt. Lett.* **2019**, *44*, 4535−4538.

(20) Baniasadi, M.; Maleki-Bigdeli, M. A.; Baghani, M. Force and Multiple-Shape-Recovery in Shape-Memory-Polymers under Finite Deformation Torsion-Extension. *Smart Mater. Struct.* **2020**, *29*, No. 055011.

(21) Jo, Y. H.; Zhou, B. H.; Jiang, K.; Li, S. Q.; Zuo, C.; Gan, H. H.; He, D.; Zhou, X. P.; Xue, Z. G. Self-Healing and Shape-Memory Solid Polymer Electrolytes with High Mechanical Strength Facilitated by a Poly(vinyl alcohol) Matrix. *Polym. Chem.* **2019**, *10*, 6561−6569.

(22) Fang, Y.; Ni, Y.; Leo, S.-Y.; Taylor, C.; Basile, V.; Jiang, P. Reconfigurable Photonic Crystals Enabled by Pressure-Responsive Shape-Memory Polymers. *Nat. Commun.* **2015**, *6*, No. 7416.
(23) Fang, Y.; Ni, Y. L.; Leo, S. Y.; Wang, B. C.; Basile, V.; Taylor, C.; Jiang, P. Direct Writing of Three-Dimensional Macroporous Photonic Crystals on Pressure-Responsive Shape Memory Polymers. *ACS Appl. Mater. Interfaces* **2015**, *7*, 23650−23659.
(24) Morphew, D.; Shaw, J.; Avins, C.; Chakrabarti, D. Programming Hierarchical Self-Assembly of Patchy Particles into Colloidal Crystals via Colloidal Molecules. *ACS Nano* **2018**, *12*, 2355−2364.
(25) Li, M.; Cao, Y. H.; Ni, X. J.; Cao, G. Q. Rapid Evaporation-Induced Self-Assembly of Three-Dimensional Photonic Crystals Using Fe3O4@C Magnetic Nanocomposites. *New J. Chem.* **2017**, *41*, 1980−1985.
(26) Jaquay, E.; Martinez, L. J.; Mejia, C. A.; Povinelli, M. L. Light-Assisted, Templated Self-Assembly Using a Photonic-Crystal Slab. *Nano Lett.* **2013**, *13*, 2290−2294.
(27) Endo, T.; Kajita, H.; Kawaguchi, Y.; Kosaka, T.; Himi, T. Label-Free Optical Detection of C-Reactive Protein by Nanoimprint Lithography-Based 2D-Photonic Crystal Film. *Biotechnol. J.* **2016**, *11*, 831−837.
(28) Song, D. P.; Zhao, T. H. H.; Guidetti, G.; Vignolini, S.; Parker, R. M. Hierarchical Photonic Pigments via the Confined Self-Assembly of Bottlebrush Block Copolymers. *ACS Nano* **2019**, *13*, 1764−1771.
(29) Kim, J. H.; Williams, S. T.; Cho, N.; Chueh, C. C.; Jen, A. K.-Y. Enhanced Environmental Stability of Planar Heterojunction Perovskite Solar Cells Based on Blade-Coating. *Adv. Energy Mater.* **2015**, *5*, No. 1401229.
(30) Pierre, A.; Sadeghi, M.; Payne, M. M.; Facchetti, A.; Anthony, J. E.; Arias, A. C. All-Printed Flexible Organic Transistors Enabled by Surface Tension-Guided Blade Coating. *Adv. Mater.* **2014**, *26*, 5722−5727.
(31) Stöber, W.; Fink, A.; Bohn, E. Controlled Growth of Monodisperse Silica Spheres in the Micron Size Range. *J. Colloid Interface Sci.* **1968**, *26*, 62−69.
(32) Yang, H.; Jiang, P. Large-Scale Colloidal Self-Assembly by Doctor Blade Coating. *Langmuir* **2010**, *26*, 13173−13182.
(33) Yang, H.; Jiang, P. Self-Cleaning Diffractive Macroporous Films by Doctor Blade Coating. *Langmuir* **2010**, *26*, 12598−12604.
(34) Deng, J.; Tao, X.; Li, P.; Xue, P.; Zhang, Y.; Sun, X.; Kwan, K. C. A Simple Self-Assembly Method for Colloidal Photonic Crystals with a Large Area. *J. Colloid Interface Sci.* **2005**, *286*, 573−578.
(35) Nucara, L.; Greco, F.; Mattoli, V. Electrically Responsive Photonic Crystals: a Review. *J. Mater. Chem. C* **2015**, *3*, 8449−8467.
(36) Dou, W.; Tan, Y. Y. Low-Voltage Self-Assembled Indium Tin Oxide Thin-Film Transistors Gated by Macroporous SiO_2 Treated by H3PO4. *RSC Adv.* **2019**, *9*, 30715−30719.
(37) Ou, Y.; Zhou, D.; Xu, Z. K.; Wan, L. S. Surface Modification of Self-Assembled Isoporous Polymer Membranes For Pressure-Dependent High-Resolution Separation. *Polym. Chem.* **2019**, *10*, 3201−3209.
(38) Huang, Y. F.; Sun, J. J.; Wu, D. H.; Feng, X. S. Layer-By-Layer Self-Sssembled Chitosan/PAA Nanofiltration Membranes. *Sep. Purif. Technol.* **2018**, *207*, 142−150.
(39) Zhao, Y.; Huang, W. M.; Wang, C. C. Thermo/Chemo-Responsive Shape Memory Effect for Micro/nano Surface Patterning Atop Polymers. *Nanosci. Nanotechnol. Lett.* **2012**, *4*, 862−878.
(40) Kim, J. H.; Lee, G. H.; Kim, J. B.; Kim, S.-H. Macroporous Hydrogels for Fast and Reversible Switching between Transparent and Structurally Colored States. *Adv. Funct. Mater.* **2020**, *30*, No. 2001318.
(41) Zhang, R.; Wang, Q.; Zheng, X. Flexible Mechanochromic Photonic Crystals: Routes to Visual Sensors and their Mechanical Properties. *J. Mater. Chem. C* **2018**, *6*, 3182−3199.

https://dx.doi.org/10.1021/acsami.0c07410
ACS Appl. Mater. Interfaces 2020, 12, 36478−36484